

Substrate- and Time-Dependent Photoluminescence of Quantum Dots Inside the Ultrathin Polymer LbL Film

Dmitry Zimmitsky,[†] Chaoyang Jiang,[†] Jun Xu,[‡] Zhiqun Lin,[‡] and Vladimir V. Tsukruk^{*,†}

School of Materials Science and Engineering, Georgia Institute of Technology, Atlanta, Georgia 30332, and Department of Materials Science and Engineering, Iowa State University, Ames, Iowa 50011

Received December 20, 2006. In Final Form: January 22, 2007

The photoluminescence of CdSe/ZnS quantum dots (QDs) in different configurations at solid surfaces (glass, silicon, PDMS, and metals) is considered for three types of organization: QDs directly adsorbed on solid surfaces, separated from the solid surface by a nanoscale polymer film with different thickness, and encapsulated into a polymer film. The complete suppression of photoluminescence for QDs on conductive metal surfaces (copper, gold) indicated a strong quenching effect. The temporal variation of the photoluminescent intensity on other substrates (glass, silicon, and PDMS) can be tuned by placing the nanoscale (3–50 nm) LbL polymer film between QDs and the substrate. The photooxidation and photobleaching processes of QD nanoparticles in the vicinity of the solid surface can be tuned by proper selection of the substrate and the dielectric nanoscale polymer film placed between the substrate and QDs. Moreover, the encapsulation of QD nanoparticles into the polymer film resulted in a dramatic initial increase in the photoemission intensity due to the accelerated photooxidation process. The phenomenon of enhanced photoemission of QDs encapsulated into the ultrathin polymer film provides not only the opportunity for making flexible, ultrathin, QD-containing polymer films, transferable to any microfabricated substrate, but also improved light emitting properties.

Introduction

Semiconductor nanocrystals, or colloidal quantum dots (QDs), show unique size-dependent optical properties¹ and are currently of great interest for various prospective applications in optoelectronic,^{2,3} photovoltaic⁴ devices, optical amplifier media for telecommunication networks,⁵ and for biolabeling.^{6,7} The good photostability, high photoluminescence (PL) intensity, and a broad emission tunability make these QDs an excellent choice as novel chromophores. Assembling QDs at solid surfaces and interfaces is a critical stage required for their integration with solid-state devices. Moreover, processing of QDs in a combination with polymeric materials may allow the fabrication of flexible and thin luminescent materials in the form of films, fibers, and 3D items. Several fabrication techniques are widely used to make ultrathin organized nanocomposite films including spin casting, Langmuir–Blodgett (LB) deposition, and layer-by-layer (LbL) assembly.^{8,9} One of the more successful approaches employed was the LbL assembly (especially spin-assisted LbL), which allows for controlled placement of various nanoparticles such as QDs between polymeric multilayers and precise adjustment of distance between the underlying surface and the array of nanoparticles confined within multilayered structures.^{10–14}

It is important to understand the effect of the supporting substrate in the emission properties of QD nanoparticles, because the photoemission can be quenched or enhanced by the substrate located in the close proximity to the QDs. As known, the decay of the quenching efficiency is highly sensitive to the distance, with the highest quenching occurring at 2–10 nm from the metal surfaces with quenching virtually disappearing for the distance higher than 10–20 nm.¹⁵ According to the Förster resonant energy transfer (FRET) theory, the energy transfer efficiency near a metal nanoparticle scales to the inverse sixth power of the distance if the nanoparticle is assumed to be a single dipole.^{16,17} However, for certain combinations of metal surfaces and chromophores, a weak distance dependence (down to linear) with significant quenching extending beyond a 20 nm gap or even an increase in emission intensity can be observed.^{18–21}

As a step in the understanding of the QD behavior at different surfaces, Kotov and his co-workers studied the formation of QDs monolayers on silicon substrates modified with different polycations: (3-aminopropyl)-triethoxysilane (APTES), polyethylenimine (PEI), and poly(diallyldimethylammonium) chloride (PDDA).²² The marked difference in the structural characteristics of the QD aggregation such as an overall particle density and the variable surface distribution has been found for these surfaces.

* Corresponding author. E-mail: vladimir@mse.gatech.edu.

[†] Georgia Institute of Technology.

[‡] Iowa State University.

(1) Warren, C. W.; Nie, S. *Science* **1998**, *281*, 5385.

(2) Schlamp, M. C.; Peng, X.; Alivisatos, A. P. *J. Appl. Phys.* **1997**, *82*, 5837.

(3) Gao, M.; Lesser, C.; Kirstein, S.; Mohwald, H.; Rogach, A. L.; Weller, H. *J. Appl. Phys.* **2000**, *87*, 2297.

(4) Barnham, K.; Marques, J. L.; Hassard, J.; O'Brien, P. *Appl. Phys. Lett.* **2000**, *76*, 1197.

(5) Harrison, M. T.; Kershaw, S. V.; Burt, M. G.; Rogach, A. L.; Kornowski, A.; Eychmuller, A.; Weller, H. *Pure Appl. Chem.* **2000**, *72*, 295.

(6) Bruchez, M. P.; Moronne, M.; Gin, P.; Weiss, S.; Alivisatos, A. P. *Science* **1998**, *281*, 2013.

(7) Han, M.; Gao, X.; Su, J. Z.; Nie, S. *Nat. Biotechnol.* **2001**, *19*, 631.

(8) Ludwigs, S.; Böker, A.; Voronov, A.; Rehse, N.; Magerle, R.; Krausch, G. *Nat. Mater.* **2003**, *2*, 744.

(9) Reece, T. J.; Ducharme, S.; Sorokin, A. V.; Poulsen, M. *Appl. Phys. Lett.* **2003**, *82*, 142.

(10) Jiang, C.; Markutsya, S.; Pikus, Y.; Tsukruk, V. V. *Nat. Mater.* **2004**, *3*, 721.

(11) Jiang, C.; Tsukruk, V. V. *Adv. Mater.* **2006**, *18*, 829.

(12) *Multilayer Thin Films*; Decher, G., Schlenoff, J. B., Eds.; Wiley-VCH: Weinheim, Germany, 2003.

(13) *Protein Architecture: Interfacial Molecular Assembly and Immobilization Biotechnology*; Lvov, Y., Möhwald, H., Eds.; Marcel Dekker: New York, 2000.

(14) Tang, Z.; Kotov, N. A. *Adv. Mater.* **2005**, *17*, 951.

(15) Bene, L. *J. Mol. Recognit.* **2005**, *18*, 236.

(16) Förster, T. *Ann. Phys.* **1948**, *2*, 55.

(17) Lakowicz, J. R. *Principles of Fluorescence Spectroscopy*; Kluwer Academic/Plenum Publisher: New York, 1999.

(18) Singamaneni, S.; Jiang, C.; Merrick, E.; Kommireddy, D.; Tsukruk, V. V. *J. Macromol. Sci., Part B: Phys.* **2007**, *46*, 7.

(19) Zucolotto, V.; Faceto, A. D.; Santos, F. R.; Mendonca, C. R.; Guimaraes, F. E. G.; Oliveira, O. N., Jr. *J. Phys. Chem. B* **2005**, *109*, 7063.

(20) Baur, J. W.; Rubner, M. F.; Reynolds, J. R.; Kim, S. *Langmuir* **1999**, *15*, 6460.

(21) Kulakovich, O.; Strelak, N.; Artemyev, M.; Stupak, A.; Maskevich, S.; Gaponenko, S. *Nanotechnology* **2006**, *17*, 5201.

(22) Tang, Z.; Wang, Y.; Kotov, N. A. *Langmuir* **2002**, *18*, 7035.

On the PDDA-coated surface, QDs were adsorbed in a homogeneous, close-packed monolayer with occasional random aggregation or multilayer formation. Unlike PDDA, a significant aggregation of QDs occurs on a PEI or APTES-modified surface with single QDs observed only occasionally. However, the effect of the thickness of the polymer/organic film on the PL intensity of QDs was not elucidated. The effect of polymer type on the PL intensity of colloidal solutions of QDs was also reported. For instance, the ZnS:Mn²⁺ QDs covered with poly(vinylbutyral) and sodium polyphosphate showed PL efficiency 10–15 times higher than that of uncovered QDs.²³ Oliveira et al. have prepared multilayered polymer/CdSe LbL composite films.²⁴ The importance of the host polymer in the LbL films was demonstrated by the observation that the PL intensity of poly(amidoamine)/CdSe films is ca. 50 times higher than the PL from PAH/CdSe films.

A very intriguing phenomenon of the photoinduced luminescence enhancement has been reported in two-dimensionally close-packed QD layers as well as in QD dispersions.²⁵ A significant increase of the intensity of QD emission upon illumination with UV or ambient light observed in this study and in several other reports opens the door for highly increased efficiency of bioimaging with QDs and thus draws significant attention.^{22,26,27} Several mechanisms underlying the PL intensity increase have been suggested in recent studies including (1) photoadsorption of gaseous molecules (e.g., H₂O) on QD surface and the resulting passivation of the surface states (photoactivation),^{26,28} (2) photoinduced surface transformation²⁹ and/or photoinduced rearrangement of ligand molecules on QD surfaces³⁰ (phototransformation), (3) photoneutralization of local charged centers inside and outside of QDs (photoneutralization),³¹ and (4) photoionization of QDs and subsequent trap filling by ejected carriers that leads to the suppression of the ionization probability of the remaining neutral QD nanoparticles (photoelectrification).^{32,33} For instance, it has been demonstrated that QD nanoparticles coated with poly(vinylbutyral) and sodium polyphosphate as well as with poly(vinyl alcohol) and methacrylic acid showed the highest increase of the luminescence quantum efficiency upon irradiation.²³ These changes were related to the UV curing of the passivating polymer shell.

It is generally accepted that water or oxygen in a combination with light (ambient or UV) is required for these photochemical reactions to become efficient. However, overall, the temporal behavior is usually complicated by many more environmental factors, such as the atmosphere composition, QD size, ligand molecule type, and substrate nature. The role of the capping molecules, polymer shells, humidity, and the presence of oxygen in the rate of the emission intensity of QD-containing films is widely debated.

In this study, we address the role of the supporting substrates and the organic environment on the evolution of the photoemission of CdSe/ZnS QD nanoparticles under UV illumination. The complete quenching of the PL intensity of the QD nanoparticles encapsulated into polymeric LbL film was observed on conductive metal surfaces (copper, gold) in a sharp contrast with the nonconductive silicon, poly dimethyl siloxane (PDMS), and glass surfaces. The placement of QDs on these surfaces leads to the significant increase of the PL intensity accompanied by the blue-shift of the main emission peak. We demonstrate that the photoemission intensity can be tuned by varying the thickness of the LbL films (within 3–50 nm) in contact with QD nanoparticles. Moreover, we observed that the higher increase in the emission intensity occurs for the QD nanoparticles encapsulated between the polymeric LbL multilayered films.

Experimental Section

Materials. The polyelectrolytes, poly(allylamine hydrochloride) (PAH) (MW = 70 000) and poly(sodium 4-styrenesulfonate) (PSS) (MW = 70 000), were purchased from Aldrich and used without further purification. Ultrapure water with a resistivity $\sigma > 18.0$ M Ω cm used in all experiments was purified with a Nanopure system. Silicon wafers were cut to a typical size of 10 × 20 mm and were cleaned in a piranha solution [1:3 (v/v) H₂SO₄/H₂O₂], according to a usual procedure adapted in our laboratory.³⁴ *Attention: Piranha solution is extremely dangerous and should be very carefully treated.* Silicon wafers of the {100} orientation with one side polished (Semiconductor Processing Co.) were atomically smooth (micro-roughness within 1 × 1 μ m surface area below 0.1 nm). After being cleaned, the substrates were rinsed thoroughly with Nanopure water and dried with dry nitrogen before they were used. PDMS substrates were prepared by curing liquid pre-polymer (Sylgard 184, Dow Chemical) on top of the corresponding silicon template at room temperature overnight under vacuum.

Synthesis of CdSe Nanoparticles. Core-shell CdSe/ZnS QDs were prepared according to the known procedure.^{35–37} An amount of ZnS precursor (diethylzinc (Zn(CH₂CH₃)₂):hexamethyl(diisilathiane) ((TMS)₂S) = 1:1 in trioctylphosphine (TOP)) was added to tri-*n*-octylphosphine oxide (TOPO)-functionalized CdSe solution at elevated temperature. The resulting organic-soluble CdSe/ZnS QDs were subsequently converted into water-soluble nanoparticles via ligand exchange with thioacetic acid (TAA) according to the usual procedure.³⁸

Fabrication and Release of LbL Films. The multilayer QD-LbL polymer films (general formula: (PAH/PSS)_{*n*}PAH/QD/(PAH/PSS)_{*n*}(PAH)) were fabricated using spin-assisted (SA)-LbL method as discussed in detail earlier.^{39–41} A monolayer of PAH on a silicon wafer was deposited from the 0.2% PAH solution by spin-casting for 20 s at 3000 rpm. The substrate was rinsed twice with Nanopure water and dried while spinning for 20 s. In the same manner, PSS monolayer was deposited from the 0.2% solution. This procedure was repeated until the needed number of polymer bilayers, *n*, was achieved. To form a QD monolayer, a 150 μ L droplet of 0.1% QD solution was dropped on the PAH-terminated silicon substrate and rotated for 20 s at 3000 rpm. The substrate was then rinsed twice with Nanopure water, and the same number of polymer bilayers, *n*, was deposited again. For the preparation of released LbL films, a sacrificial cellulose acetate (CA) layer was spin cast on the freshly

(23) Bol, A. A.; Meijerink, A. *J. Phys. Chem. B* **2001**, *105*, 10203.

(24) Zucolotto, V.; Gatta's-Asfura, K. M.; Tumolo, T.; Perinotto, A. C.; Antunes, P. A.; Constantino, C. J. L.; Baptista, M. S.; Leblanc, R. M.; Oliveira, O. N., Jr. *Appl. Surf. Sci.* **2005**, *246*, 397.

(25) Kimura, J.; Uematsu, T.; Maenosono, S.; Yamaguchi, Y. *J. Phys. Chem. B* **2004**, *108*, 13258.

(26) Cordero, S. R.; Carson, P. J.; Estabrook, R. A.; Strouse, G. F.; Buratto, S. K. *J. Phys. Chem. B* **2000**, *104*, 12137.

(27) Nazzal, A. Y.; Qu, L. H.; Peng, X. G.; Xiao, M. *Nano Lett.* **2003**, *3*, 819.

(28) Simurda, M.; Nemecek, P.; Trojaneck, F.; Maly, P. *Thin Solid Films* **2004**, *453–454*, 300.

(29) Hess, B. C.; Okhrimenko, I. G.; Davis, R. C.; Stevens, B. C.; Schulzke, Q. A.; Wright, K. C.; Bass, C. D.; Evans, C. D.; Summers, S. L. *Phys. Rev. Lett.* **2001**, *86*, 3132.

(30) Jones, M.; Nedeljkovic, J.; Ellingson, R. J.; Nozik, A. J.; Rumbles, G. *J. Phys. Chem. B* **2003**, *107*, 11346.

(31) Oda, M.; Shen, M. Y.; Saito, M.; Goto, T. *J. Lumin.* **2000**, *87–89*, 469.

(32) Maenosono, S.; Dushkin, C. D.; Saita, S.; Yamaguchi, Y. *Jpn. J. Appl. Phys., Part 1* **2000**, *39*, 4006.

(33) Maenosono, S. *Chem. Phys. Lett.* **2003**, *376*, 666.

(34) Tsukruk, V. V.; Bliznyuk, V. N. *Langmuir* **1998**, *14*, 446.

(35) Peng, X.; Manna, L.; Yang, W. D.; Wickham, J.; Scher, E.; Kadavanich, C.; Alivisatos, A. P. *Nature* **2000**, *404*, 59.

(36) Xu, J.; Xia, J.; Wang, J.; Shinar, J.; Lin, Z. *Appl. Phys. Lett.* **2006**, *89*, 133110.

(37) Xu, J.; Xia, J.; Lin, Z. Q. *Angew. Chem., Int. Ed.* **2007**, *46*, 1860.

(38) Chan, W. C. W.; Nie, S. *Science* **1998**, *281*, 2016.

(39) Lvov, Y.; Decher, G.; M6hwald, H. *Langmuir* **1993**, *9*, 481.

(40) Decher, G. *Science* **1997**, *277*, 1232.

(41) Tang, Z.; Kotov, N. A.; Magonov, S.; Ozturk, B. *Nat. Mater.* **2003**, *2*, 413.

cleaned silicon substrate.^{10,11,42} A droplet (150 μL) of the 2% CA acetone solution containing 1 wt % of water was placed on the silicon substrate and rotated for 20 s with a 3000 rpm. The LbL multilayer was further assembled on top of the sacrificial CA layer.

Substrate cleaning, fabrication, and release of LbL films were performed in a cleanroom class 100. After fabrication, the LbL films were cut into approximately $2 \times 2 \text{ mm}^2$ squares using a stainless steel microneedle and released by submersion in acetone, which dissolves the CA layer.⁴³ The LbL films were next transferred to Nanopure water where they were picked up with various solid substrates and dried before use. Drying and removing a water layer results in significant residual stresses, which, however, do not affect the film state as was discussed in previous studies.¹⁰ In this study, we used a highly polished copper plate with a single micromachined hole in its center, a freshly clean silicon wafer, a PDMS substrate with/without sputtered gold, a copper transmission electron microscopy (TEM) grid, and a float glass slide.

Instrumentation. UV-vis spectra were recorded with a UV-1601 spectrometer (Shimadzu). AFM images were collected using a Dimension 3000 AFM microscope (Digital Instruments) in the tapping mode according to the usual procedure adapted in our laboratory for ultrathin polymer films.⁴⁴ To evaluate a film thickness, the LbL film edge was scanned with AFM, and the images were analyzed with the bearing analysis. TEM was done with a JEOL 1200EX electron microscope operated at 80 kV. Bright field optical and fluorescent images were captured with an optical fluorescent microscope Leica DM4000M (an excitation wavelength 365 nm). Luminescence spectra were recorded using a Craig QDI 202 point-shot spectrophotometer attached to the microscope (sampling area $1 \times 1 \mu\text{m}$, collection time 15 s). UV illumination of LbL-QDs films was conducted with the optical setup of optical fluorescent microscope Leica DM4000M. A mercury lamp (100 W) was used as a light source. The light with wavelength 365 nm was focused using a $50\times$ objective (N.A. 0.6) onto the sample with the diameter of the beam spot $500 \mu\text{m}$. The intensity of the incident light was estimated to be about 1.3 W cm^{-2} .

Buckling Test. The buckling test was conducted for the evaluation of the elastic modulus of LbL films.^{45,46} For an isotropic film, a uniform buckling pattern having a characteristic wavelength, λ , takes place above a critical compressive stress, and this spacing can be used to evaluate the elastic modulus.⁴⁷ To initiate the buckling pattern, a $2 \times 2 \text{ mm}$ LbL film was placed over a $0.6 \times 0.6 \text{ cm} \times 0.4 \text{ cm}$ PDMS substrate, which was slowly compressed with a micrometer-sized increment keeping the compressive strain below 2%. The compression was monitored in a differential interference contrast (DIC) mode adjusted for maximum contrast. Digital optical images were analyzed by using Fourier transformation within ImageJ software.

Results and Discussion

QD Properties. QD solution shows an adsorption maximum at 590 nm, which corresponds to the first excitonic transition in the absorption spectra (Figure 1).⁴⁸ The corresponding photoemission displays a pronounced and narrow PL peak at 633 nm, which is common for CdSe nanoparticles with a 5 nm diameter (Figure 1).⁴⁹ The general schematic of water-soluble CdSe/ZnS nanoparticles capped with TAA is shown in Figure 2. The analysis of QD size distribution was reported in our recent paper.⁵⁰ Briefly, QDs show a relatively narrow distribution with the average

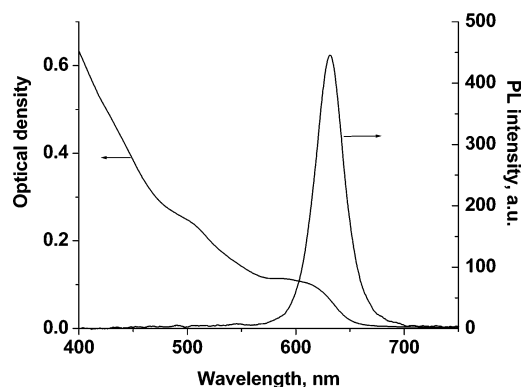


Figure 1. Absorption and luminescence spectra of 0.1% QD solution.

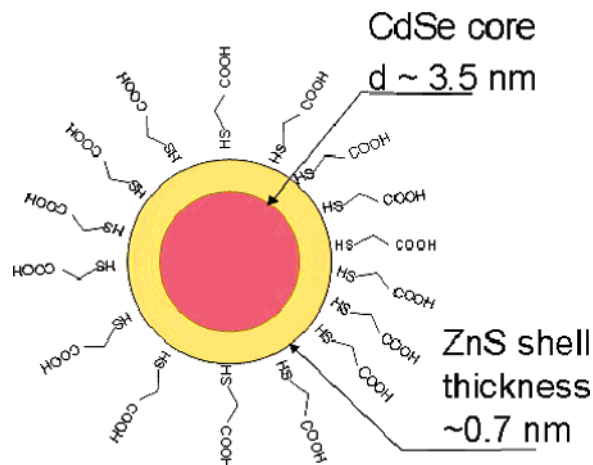


Figure 2. General schematic of water-soluble TGA capped CdSe/ZnS quantum dot.

diameter at $4.9 \pm 1.2 \text{ nm}$. The CdSe core is covered with two to three atomic layers of ZnS, which correspond to the thickness of ZnS shell of about 0.7 nm.³⁶ The surface density of QDs was kept fairly constant in the course of deposition for all experiments: around 3000 particles per $1 \mu\text{m}^2$, which corresponded to the surface coverage 6% (see TEM data in Figure 3a and detailed discussion in ref 50). The high-resolution AFM image shows predominantly individual nanoparticles deposited on the solid surface (lateral dimensions significantly dilated due to the convolution with the AFM tip) (Figure 3b). The QD surface density was kept relatively low due to a tendency to the formation of QDs aggregates with the increasing surface coverage.

In our study, we consider the QDs on different stages of their encapsulation into LbL film: (a) on the top of the silicon surface covered with the PAH monolayer (a reference specimen), (b) separated from the silicon surface by nanoscale LbL films (thickness varied from 3 to 50 nm), and (c) encapsulated inside the LbL films with a variable thicknesses (Figure 4). The LbL technique allows a precise control of the QD placement relatively to the silicon surface with QD nanoparticles predominantly confined into a single plane effectively forming loose monolayer. The thickness of PAH/PSS bilayers in our experiments ranged between 2.5 and 3 nm, which is common for this composition.⁵¹

QD Photoemission with Different Configurations. As we observed, the photoemission intensity of QD monolayer on the silicon surface strongly depends upon the thickness of the underlying polymeric film (Figure 5a). However, the position of

(42) Jiang, C.; Markutsya, S.; Shulha, H.; Tsukruk, V. V. *Adv. Mater.* **2005**, *17*, 1669.

(43) Mamedov, A. A.; Kotov, N. A. *Langmuir* **2000**, *16*, 5530.

(44) Tsukruk, V. V. *Rubber Chem. Technol.* **1997**, *70*, 430.

(45) Xiong, Y.; Xie, Y.; Wu, C.; Yang, J.; Li, Z.; Xu, F. *Adv. Mater.* **2003**, *15*, 405.

(46) Sun, X.; Li, Y. *Adv. Mater.* **2005**, *17*, 2626.

(47) Park, J.-H.; Oh, S.-G.; Jo, B.-W. *Mater. Chem. Phys.* **2004**, *87*, 301.

(48) Andreev, A. D.; Datsiev, R. M.; Seisyan, R. P. *Phys. Status Solidi B* **1999**, *215*, 325.

(49) Medintz, I. L.; Uyeda, H. T.; Goldman, E. R.; Mattoussi, H. *Nat. Mater.* **2005**, *4*, 435.

(50) Zimnitsky, D.; Jiang, C.; Xu, J.; Lin, Z.; Zhang, L.; Tsukruk, V. V. *Chem. Mater.*, submitted.

(51) Gunawidjaja, R.; Jiang, C.; Ko, H.; Tsukruk, V. V. *Adv. Mater.* **2006**, *18*, 2895.

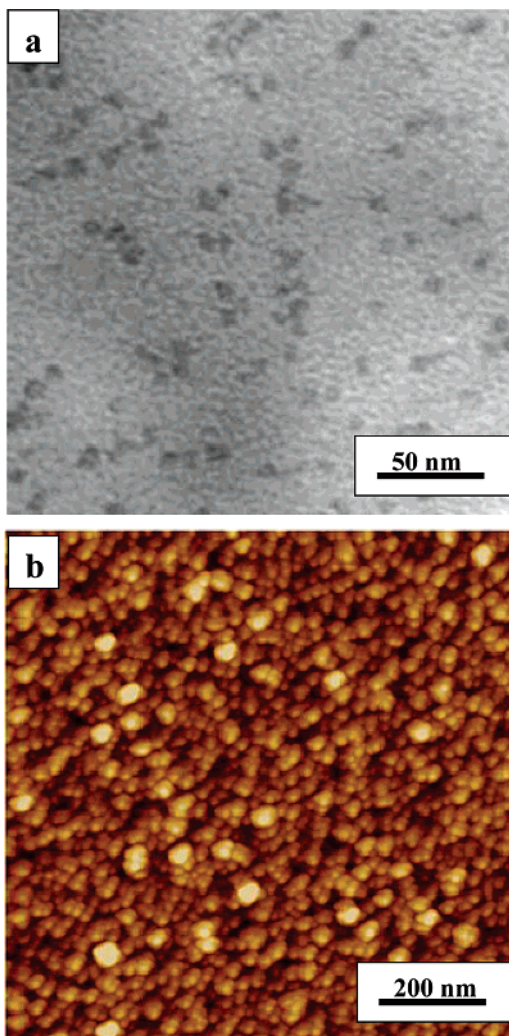


Figure 3. TEM (a) and height AFM (b) images of CdSe nanoparticles encapsulated in (a) and adsorbed on (b) LbL film.

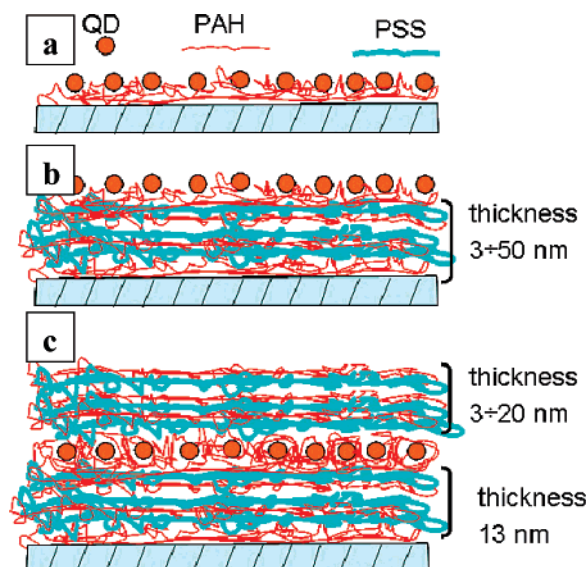


Figure 4. General schematic of the microstructure of the QD monolayer located (a) on top of PAH-covered silicon surface, (b) on top of the LbL film, and (c) encapsulated between two LbL films.

the PL maximum remains unchanged, indicating identical local environment (PAH surface in all cases). The PL intensity linearly increases with the increasing thickness of the underlying polymer

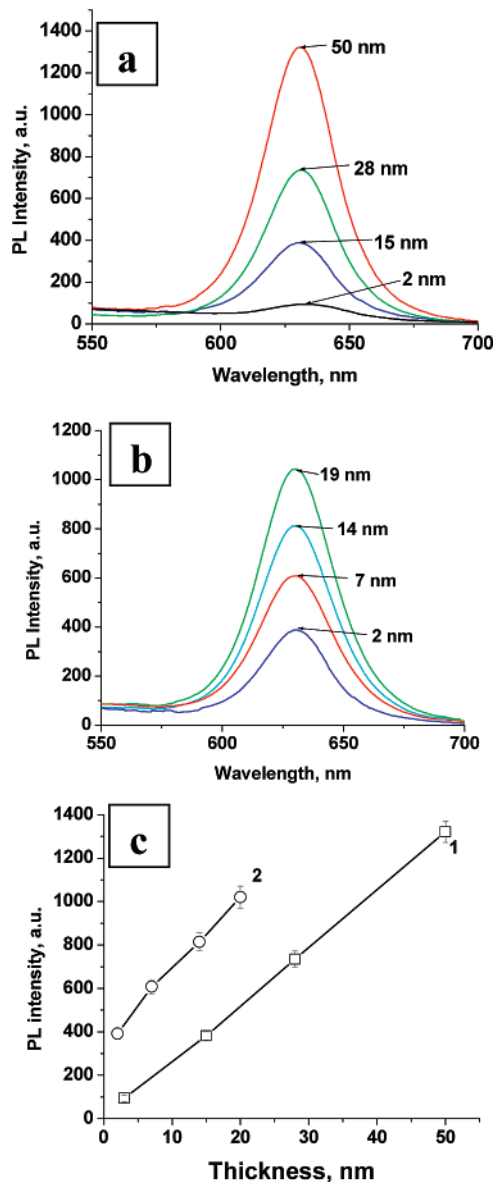


Figure 5. Emission spectra of the LbL films with different thickness of polymer film between QDs and silicon surface (a) and above QD monolayer (b). The PL intensity versus the thickness of polymer LbL film: 1 for (a) and 2 for (b), (c).

film manifold for the same experimental conditions (10 times for the film thickness 50 nm) (Figure 5c). Similarly, adding the polymer film on top of QDs leads to a linear increase of photoemission intensity with a further, 2-/3-fold increase as compared to uncapped QDs (Figure 5b,c).

The increase of the PL intensity with the increasing distance between QD and the silicon surface can be related to the reduction of the energy transfer between QD nanoparticles and the silicon surface. The presence of conducting and semiconducting surfaces in close proximity is known to be responsible for the quenching of the QD photoemission.⁵⁴ The effect of quenching of fluorescence of organic dyes and fluorescent nanoparticles by metal surfaces is known for fluorophores located within 5–10

(52) Duijs, E. F.; Findeis, F.; Deutschmann, R. A.; Bichler, M.; Zrenner, A.; Abstreiter, G.; Adlkofer, K.; Tanaka, M.; Sackmann, E. *Phys. Status Solidi B* **2001**, *224*, 871.

(53) Wang, C. F.; Badolato, A.; Wilson-Rae, I.; Petroff, P. M.; Hu, E. *Appl. Phys. Lett.* **2004**, *85*, 3423.

(54) Borges, C. A. M.; Rodrigues, C. A.; Faria, R. M.; Giumaraes, F. E. G. *Synth. Met.* **2005**, *154*, 133.

nm from the surfaces.^{52,53} However, the surprising result is that the surfaces act as an effective emission quencher on the distances as high as 30 nm if PSS-PAH films are involved. We suggest that these polycation-polyanion multilayers used in our study act as a charge conductor between QDs and the metal surface, on one hand, and between adjacent QD nanoparticles, on the other hand. As a result, QDs form a network, and the energy, absorbed by QDs, effectively dissipates within polyelectrolyte matrix with substantial water content without photoemission. In fact, adding PAH/PSS bilayers was demonstrated as an effective way to reduce photoemission quenching of organic chromophores.¹⁸ In all cases, the distance dependence is much slower than that predicted by different energy transfer models, which is not clear understood and might be associated with the in-plane redistribution of initiating centers as mentioned above.¹⁸

The increasing photoemission intensity after the capping of QDs with LbL film was unexpected because the distance between the silicon surface and QDs remains constant. We might speculate that this phenomenon can be caused by specific interactions of QDs with polymer matrix. Wrapping of QDs with charged polyelectrolyte backbones could result in the partial healing of the existing surface defects due to slow oxidation of QDs core within swollen matrix during and after deposition of additional bilayers from aqueous media.⁵⁵ In fact, water molecules adsorbed on the QD surface were considered to be instrumental in the photoemission activation.²⁶ Other study reported that the PL intensity of QDs in colloidal solution can be significantly enhanced by adding proper polymers.²³ It has been suggested that the coverage of QDs by polymer chains reduces the number of dangling bonds on the surface of the particle. Dangling bonds provide surface trap states for nonradiative recombination, and their reduction effectively suppresses the energy transfer responsible for the reduced photoemission.⁵⁵ In a related study, Zhang et al. observed the increase of the PL intensity of QDs in the presence of poly(acrylic acid).⁵⁶ The authors considered the wrapping of polymer chains around the fluorescent nanocrystals as a protective environment, improving the stability of QDs.

Effect of Substrate on the PL Intensity of Encapsulated QDs. The LbL films with encapsulated QDs were stable and robust in acetone solution, thus allowing the transfer to different solid substrates and even suspension across the microscopic opening. The results of the buckling test of these films confirmed their excellent mechanical properties with the ability to sustain high mechanical stresses. The Young's modulus estimated from the buckling periodicity according to the known approach was about 2.0 GPa.^{57,58} This value is close to those obtained earlier in our group for purely polymeric PSS-PAH LbL films, which is expected because of a very low volume content of QD nanoparticles in the LbL film tested (0.3 vol %).⁵⁹⁻⁶¹

The fabricated (PAH/PSS)₉PAH/QD/(PAH/PSS)₉PAH (QD-LbL or 9QD9) films were transferred on different substrates including silicon and PDMS, copper plates, TEM grid, glass,

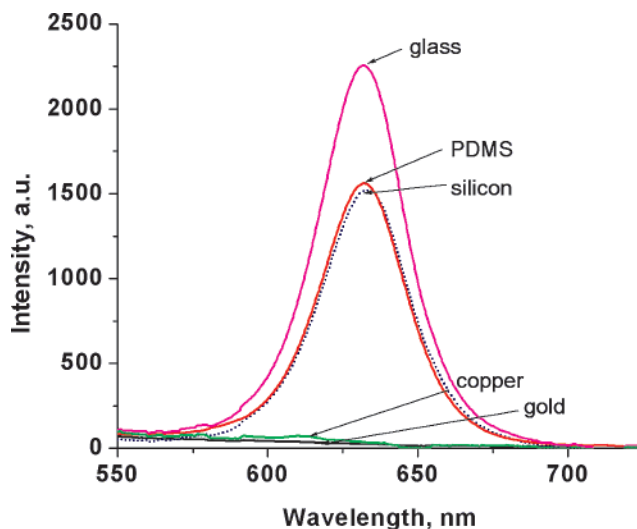


Figure 6. Emission spectra of the 9QD9 film deposited on different substrates.

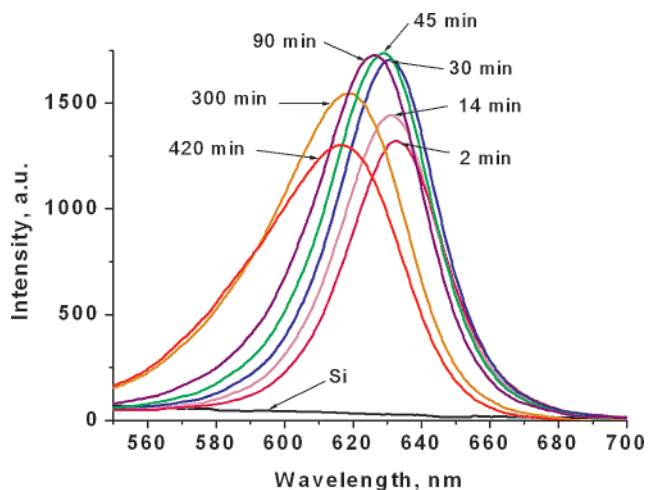


Figure 7. Emission spectra of the 9QD9 film on the silicon surface after various times of UV illumination.

and PDMS with a layer of gold. The PL peak positions of LbL films on the different substrates are very similar to that recorded for the QD solution, but the peak intensity was strongly affected by the substrate type (Figure 6). The photoemission is completely absent for the QD-LbL films transferred on metal substrates (copper and gold) (Figure 6). However, the films transferred on silicon, PDMS, and glass substrates possess strong photoemission with the intensity on glass 40% higher than that on silicon and PDMS substrates (Figure 6). The lower emission for the QD-LbL film on silicon and PDMS substrates is presumably caused by different reflective properties.

Temporal Changes of QD Photoemission upon Illumination. The temporal evolution of the PL intensity was studied for the LbL film with encapsulated QD nanoparticles deposited on selected substrates under continuous UV illumination with the intensity reaching 1.3 W cm^{-2} (Figure 7). A significant initial increase of the PL intensity occurs with 45 min of illumination followed by its gradual decrease within several hours (Figure 8a). This non-monotonic change of the PL intensity is accompanied by a steady blue-shift of the peak position (Figure 8b). The overall trend in the PL evolution is similar for LbL films deposited on different substrates although with some noticeable differences as will be discussed below.

Several recent studies revealed the temporal evolution of the PL intensity of QDs under illumination with UV and ambient

(55) Gallagher, D.; Heady, W. E.; Racz, J. M.; Bhargava, R. N. *J. Mater. Res.* **1995**, *10*, 870.

(56) Zhang, H.; Zhou, Z.; Liu, K.; Wang, R.; Yang, B. *J. Mater. Chem.* **2003**, *13*, 1356.

(57) Nolte, A. J.; Rubner, M. F.; Cohen, R. E. *Macromolecules* **2005**, *38*, 5367.

(58) Stafford, C. M.; Harrison, C.; Beers, K. L.; Karim, A.; Amis, E. J.; VanLandingham, M. R.; Kim, H.-C.; Volksen, W.; Miller, R. D.; Simonyi, E. E. *Nat. Mater.* **2004**, *3*, 545.

(59) Jiang, C.; Singamaneni, S.; Merrick, E.; Tsukruk, V. V. *Nano Lett.* **2006**, *6*, 2254.

(60) Jiang, C.; Rybak, B. M.; Markutsya, S.; Klatidis, P. E.; Tsukruk, V. V. *Appl. Phys. Lett.* **2005**, *86*, 121912.

(61) Markutsya, S.; Jiang, C.; Pikus, Y.; Tsukruk, V. V. *Adv. Funct. Mater.* **2005**, *15*, 771.

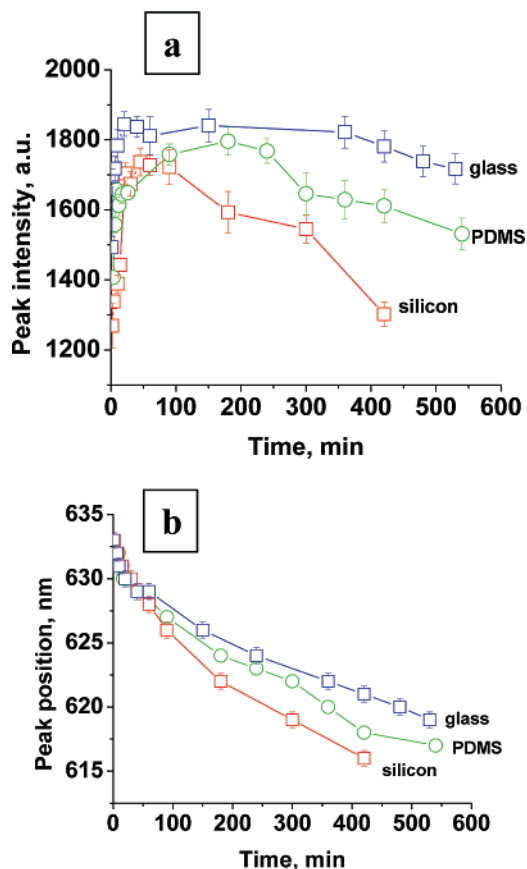


Figure 8. Evolution of intensity (a) and position (b) of emission maximum under UV illumination for 9QD9 film on silicon (1), PDMS (2), and glass (3) substrates.

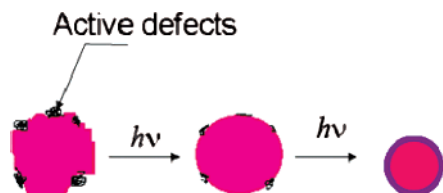


Figure 9. Schematic of nanoparticles changes under UV illumination according to the literature data. In the first stage, the number of surface defects and roughness decreases, resulting in photoemission increase. In the second stage, QD size decreases due to photobleaching, resulting in the intensity decrease.

light.^{26,62,63} Depending upon the illumination intensity and time, either continuous, steady emission increase or initial increase followed by decrease was reported. The rate of PL changes detected in different studies varied significantly because different light sources were used. The effect of environmental factors (humidity, oxygen, and wrapping polymers) on the PL evolution was demonstrated and discussed in terms of various photoinitiated processes.

The initial increase of the PL intensity of the QD nanoparticles is considered to be caused by the accelerated photooxidation of CdSe surface, which reduces the surface roughness of nanoparticles and atomic-scale surface imperfections (Figure 9).⁶² These changes result in the enhanced emission due to the reduced paths for the nonradiating energy transfer. It was demonstrated that oxygen and water molecules are critical for the initiation of

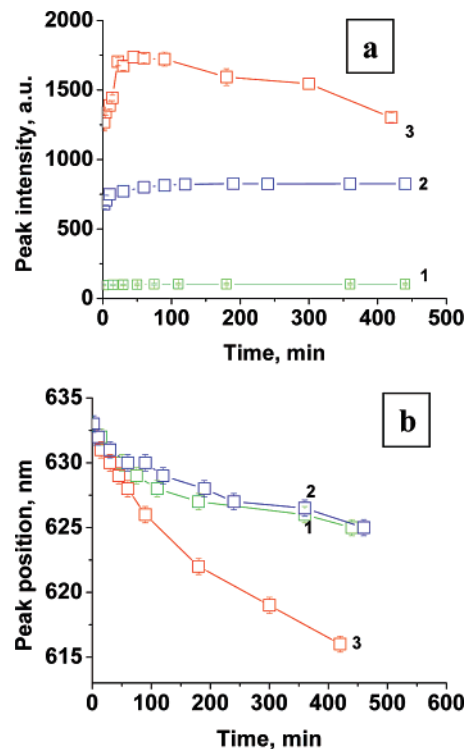


Figure 10. Evolution of intensity (a) and position (b) of emission maximum under UV illumination for QDs monolayers located on the top of PAH monolayer (1), 9QD film (2), and 9QD9 film (3). Supporting substrates were silicon wafers in all cases.

the photooxidation process. The increase of their content leads to the increase of the rate of the PL enhancement. The progressive photooxidation is further accompanied by the reduction of the QD dimensions on later stages, which results in the gradual blue-shift of the emission maximum (Figure 9). Finally, the subsequent decrease of the PL intensity under further illumination is believed to be caused by the photobleaching of QDs, which involves either thiol-shell photooxidation or the oxidation of the QDs core with a singlet oxygen.^{64–66}

Although the overall changes in the photoemission observed here are similar to those already presented in the literature, two features should be noted. First, the rate of the photooxidation decreases in the series of different substrates: silicon – PDMS – glass. We suggest that this is caused by different reflective properties of the substrates causing different amounts of light reaching QD nanoparticles. In the case of silicon wafers, the incident light reflects from the highly polished silicon surface and contributes significantly to the QD photooxidation, resulting in much faster photobleaching and diminishing nanoparticle dimensions. On the contrary, the glass substrate is the most transparent among substrates, causing the light to pass through with no additional photooxidation by the reflective light and, thus, the slowest rate of photobleaching and the size reduction. The properties of the PDMS substrate are between highly reflective silicon and transparent glass, so the rate of photooxidation of the QD-LbL film on the PDMS substrate is between silicon and glass.

Second, the evolution of the PL intensity of QDs strongly depends upon their location with respect to the substrate and their nearest polymer environment as represented in Figure 4.

(62) Wang, Y.; Tang, Z.; Correa-Duarte, M. A.; Pastoriza-Santos, I.; Giersig, M.; Kotov, N. A.; Liz-Marzan, L. M. *J. Phys. Chem. B* **2004**, *108*, 15461.

(63) Komaralal, V. K.; Rakovich, Y. P.; Bradley, A. L.; Byrne, S. J.; Corr, S. A.; Gun'ko, Y. K. *Nanotechnology* **2006**, *17*, 4117.

(64) Ma, J.; Chen, J.-Y.; Guo, J.; Wang, C. C.; Yang, W. L.; Xu, L.; Wang, P. N. *Nanotechnology* **2006**, *17*, 2083.

(65) Gao, X. H.; Nie, S. M. *Trends Biotechnol.* **2003**, *21*, 371.

(66) Zhang, Y.; He, J.; Wang, P.-N.; Chen, J.-Y.; Lu, Z.-J.; Lu, D.-R.; Guo, J.; Wang, C.-C.; Yang, W.-L. *J. Am. Chem. Soc.* **2006**, *128*, 13396.

To address this aspect, we monitored the PL intensity evolution for all three arrangements on the silicon substrate (Figure 10). In fact, very insignificant variation of the low PL intensity was observed for QDs placed in close proximity to the silicon surface (Figure 10). The separation of QDs from the silicon substrate with the polymer film resulted in the overall increase of the PL intensity, but the photooxidation rate does not change significantly. However, the encapsulation between polymeric films leads to significant initial PL enhancement followed by a gradual PL decrease. These changes are accompanied by a significant blue-shift, indicating a fast reduction of the QD nanoparticle dimension. In fact, the TEM data showed slightly reduced (10%) size of QDs in the film after illumination with UV light (not shown). Apparently, the encapsulation of QDs into the polymer film stimulates both photooxidation and photobleaching processes. This acceleration could be related to the presence of water molecules bound to polyelectrolyte matrix in the course of assembly on QD nanoparticles, as well as to the presence of the charged groups serving as additional nucleation sites.

In conclusion, we demonstrated that the photooxidation and photobleaching of QD nanoparticles in the vicinity of the solid

surface can be tuned by a proper selection of substrates and the dielectric nanoscale polymer film placed between the substrate and QDs. Moreover, the encapsulation of QD nanoparticles into the nanoscale polymer LbL films results in the dramatic increase in the photoemission intensity due to accelerated photooxidation process. The phenomenon of the enhanced photoemission of QDs encapsulated into the ultrathin polymer film is interesting for sensing purposes because such an encapsulation not only provides the opportunity for making flexible ultrathin films, transferable to any microfabricated substrate, but also leads to potentially much improved light emitting properties.

Acknowledgment. This work was supported by the AFOSR, FA9550-05-1-0209, and NSF-CTS-0506832 grants, and the 3M Non-tenured Faculty Award (Z.L.). J.X. thanks the Institute for Physical Research and Technology of Iowa State University for a Catron graduate research fellowship. We also thank Maryna Ornatska for technical assistance.

LA0636917